



Application of partial differential equation (PDE) and integral calculus to rock forming minerals

Achuenu Ifeanyi^{1*}, Lekmang C. Isah², Hyeladi Dibal², Geoffrey Mica Kumleng³

¹Department of Mining Engineering, University of Jos, Nigeria

²Department of Geology, University of Jos, Plateau State, Nigeria

³Department of Mathematics, University of Jos, Plateau State, Nigeria

Received: 03-09-2025

Revised: 11-03-2026

Accepted: 16-03-2026

DOI:

<https://doi.org/10.56566/sigmamu.v4i1.428>

Abstract: Chemical reaction in Magma is very complex, because of several anionic and cationic substitutions of different size and charge in the magma and in this case, complex problems require complex solutions. This research was focused on bridging the gap between Bowen and Goldschmidt concepts concerning the problem of elemental substitution and distribution of chemical elements in rocks throughout the time of crystallization with mathematical foundation under thermodynamic change such as Calculus, comprises differentiation, Integration, Cauchy-Riemann equation, Laplace equation and Power series comprises Euler series and Taylor series were applied to predict major minerals encompass the olivine, pyroxene, amphibole, mica, and feldspar, and their associated rocks encompass granite, basalt, andesite, and trachyte and were applied to resolve the problems of rock forming minerals in magma. Findings have shown that, in mathematical context, Bowen's and Goldschmidt rules were mathematically connected using the Mathematical formulae as;

$$\frac{\delta z}{\delta x} = \lim_{\delta x \rightarrow 0} \frac{f(x,y+dx,y) - f(x,y)}{\delta x}, \quad \text{and}$$

$$\frac{\delta z}{\delta y} = \lim_{\delta y \rightarrow 0} \frac{f(x,y+dy) - f(x,y)}{\delta y}$$

Finally the "mathematical connection" between Bowen's and Goldschmidt concepts was used in this research for a concise explanation of rock forming minerals from the beginning to the end of crystallization and would help the 'beginners' especially students of Earth sciences such as Geology, Mineralogy, Petrology and other chemical sciences such as Chemistry.

Keywords: Application; Integral Calculus; Partial Differential Equation (PDE)

Introduction

Magma \mathfrak{B} . Calculus has been used to solve engineering and scientific problems, such as mechanical, electrical, Civil, physics, and chemistry, but not much has been done using calculus, to solve geological, mineralogical & petrologic problems. The reaction processes using Bowen's and Goldschmidt rules were called Polymerization and Isomorphous (Krivyakina et al., 2023). Since all silicate minerals fall within the space of Pascal triangle, the formation of minerals from melt under thermodynamic condition obeys Cauchy's definition of sequence throughout the time of crystallization and therefore all mineral have limiting values and are convergent at certain point from $\eta = n \rightarrow p$ ($e_z \rightarrow \eta_z$) in a complex plane of magma (Harnett et al., 2019). Each of these magma domains of convergence represents a magma fraction from which crystal nucleation takes

*Corresponding Author Email: achuenuifeanyi@gmail.com

place and the resultant crystallization is called fractionation and the sequences of the repeated fractions are called fractional crystallization. Therefore, Cauchy-Riemann conditions must be satisfied at each point $Z-Z_0$ in each domain of magma \mathfrak{M} , such that Z , represents a point in which x and y are variable in Z – plane of Magma, \mathfrak{M} . Z is called a function of two variables x and y if Z has one definite value for every pair of values of values of x and y as $Z = f(x, y)$. The variables x and y are called independent variables, which Z , is called the dependent variable. Finally, the mathematical process, in which minerals Z , crystallized from the magma, \mathfrak{M} and melted back into the homogeneous magma \mathfrak{M} when heated is called CALCULUS in petrology and mineralogy that is differentiation and integration in magma \mathfrak{M} . Geochemistry and Petroleum Geology to have clear understanding of rock forming minerals from the Resident magma (\mathfrak{R}) (Abd El-Fatah et al., 2023); (De Souza et al., 2024); (Mourey & Shea, 2019)

Bowen's reaction principle, first propounded in 1928 by Norman Bowen, which explains how mineral can respond to changing equilibrium conditions when a magma is cooled, by either a continuous diffusing – controlled exchange of elements with the magma or discontinuous melting of the material. (Zubatyyuk et al., 2021), (Racioppi et al., 2024), proposed his Classical general rules to explain the distribution of the elements, in which ions of similar size and charge substitute themselves. (Leung et al., 2023); (Sessa & Rahm, 2022), proposed the complementary use of the concept of electronegativity in order to understand the distributions of the chemical elements that could not be explained completely with the Goldschmidtian rules, especially when the minerals being investigated had high percentages of covalent bonding. (Sproul, 2020), proposed that the three principal factors (ionic size, Ionic charge and electronegativity) be expressed in a single function that would not result in the dichotomous predictions. (Chen-Charpentier, 2024); (Murugesh et al., 2025), rules 2 and 3, that the site has a preferred radius of Ion (r) which enters mostly easily, for ions of the same charge, those which are closest in radius to enter most easily, ions which are larger or smaller are discriminated against (Peters et al., 2020); (Lancellotti et al., 2024).

According to Balogun Ometere Deborah, Oluwafemi Israel (Gutierrez-Navarro & Lopez-Aguayo, 2018) who reviewed Adams-Bashforth method for numerical solution of first order ordinary differential equations and used it to solve first order ordinary differential equation for the field of physical science and Engineering especially the population growth. The Adams - Bashforth methods were designed by John Couch Adams to solve a differential equation modelling capillary action due to Francis (Hetmaniok & Pleszczyński, 2022), and Adams' numerical method3.0:

Method

Mathematical Methods

Mathematical methods such as Calculus, comprises differentiation, Integration, Cauchy-Riemann equation, Laplace equation and Power series comprises Euler series and Taylor series are applied to predict major minerals encompass the olivine, pyroxene, amphibole, mica, and feldspar, in their associated rocks encompass granite, basalt, andesite, and trachyte. These mathematical methods are also used to resolve the problem of elemental substitution and distribution of chemical elements in rock throughout the time of crystallization from the beginning to the end of crystallization.

Given that;

$$\sum_{p=n}^{\eta} \binom{\eta}{p} [\beta - \alpha]^{\eta} \cdot e^x = [\beta_{\eta-p} \alpha_p] Z_0 \quad (1)$$

Where Z_0 is the silicate identity and

$$\eta = \frac{z^-}{x^+} \text{ (ionic species)}$$

' η ' is the strength of the magma \mathfrak{M} , which is the ratio of the silicate radical z^- to that of cation x^+ under electrolytic condition and ' p ' is the recipient cation which depends on ' η '.

$\binom{n}{p}$ Is the coefficient of rock forming minerals and it determines the number of outcomes of each mineral in the melt $\mathfrak{M}(Z_0)_\delta$.

Result and Discussion

Differentiation of major Rock Forming Minerals during crystallization under thermodynamic change (Δ)

The General formula used in differentiating major rock forming minerals during crystallization of Magma \mathfrak{M}_n , is shown in equation (1);

$$\sum_{p=n}^{\eta} \binom{\eta}{p} [\beta - \alpha]^n \cdot e^x = [\beta_{\eta-p} \alpha_p] Z_0 \dots\dots\dots (1)$$

$$f(Mm)^\eta = (\beta + i\alpha)^\eta \cdot e^x \dots\dots\dots (2)$$

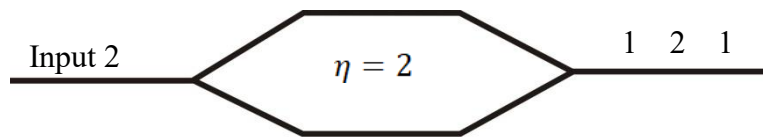
$$f(Z)^\eta = (\beta + i\alpha)^\eta \cdot e^x \dots\dots\dots (3)$$

$$Z = \beta + \alpha$$

$$\begin{cases} \beta = \text{Mg, Ca} \\ \alpha = \text{Fe, Ca} \end{cases}$$

All minerals especially silicate minerals have their derivatives in Pascal Triangle, with Z_0 , representing silicate identity which is mathematically represented as e^x .

All the rock forming minerals to be derived from the melt, $\mathfrak{B} \rightarrow \mathfrak{M}$, are the : Olivine - Pyroxene series; Amphibole Series; Mica Series; Plagioclase series; Olivine series $(\beta + i\alpha)^\eta \cdot e^x = (\beta_{\eta-p} \alpha_p) e^{Z_0}$. When you input the value of " η " in the formula $(\beta + i\alpha)^\eta \cdot e^x$, then the derivatives of $(\beta_{\eta-p} \alpha_p) e^{Z_0}$ would be generated in the pascal triangle. Therefore when you input "2"; as ' η ', then the derivatives of olivine series would be generated in the Pascal triangle as (1, 2, 1)



$$f(Z^2) e^x = (\beta^2 + 2\alpha\beta i + i\alpha^2) e^{Z_0} \dots\dots\dots (4)$$

$$\frac{\delta f}{\delta z} (e^x) = (\beta^2 + 2\alpha\beta i + i\alpha^2) e^{Z_0}$$

$$\frac{\delta f}{\delta z} (e^x) = [\text{Mg}_2 + 2i\text{MgFe} + i\text{Fe}_2] e^{Z_0}$$

$$\left(\frac{\delta f}{\delta z}\right) e^x = [\text{Mg}_2 + 2i\text{MgFe} + i\text{Fe}_2] e^{Z_0}$$

$$e^{Z_0} = \text{SiO}_4$$

$$\frac{\delta f}{\delta z} (\text{SiO}_4) = \text{Mg}_2\text{SiO}_4 + 2i\text{MgFeSiO}_4 + i\text{Fe}_2 \text{SiO}_4$$

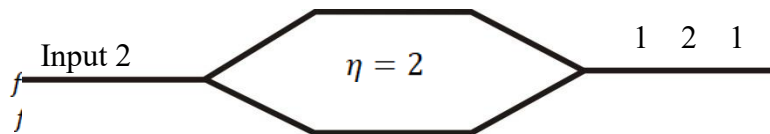
$$\frac{\delta f}{\delta z} (\text{SiO}_4) = \text{Mg}_2\text{SiO}_4 + i(2\text{MgFeSiO}_4) + i\text{Fe}_2 \text{SiO}_4 \dots\dots\dots (5)$$

$$f(Z^2) e^{Z_0} = \text{Forsterite} + \text{Olivine} + \text{Fayalite}$$

Equation (5) above represents the derivatives of olivine series in Pascal triangle.

Pyroxene Series $(\beta + i\alpha)^\eta \cdot e^x = (\beta_{\eta-p} \alpha_p) e^{Z_0}$.

When you input 2 in the formula $(\beta + i\alpha)^\eta \cdot e^x$ then the derivatives of olivine series would be generated as (1 2 1) in the Pascal triangle.



$$\frac{\delta f}{\delta z} = \text{Mg}_2 + 2i\text{MgFe} + i\text{Fe}_2$$

$$\left(\frac{\delta f}{\delta z}\right) e^x = [\text{Mg}_2 + 2i\text{MgFe} + i\text{Fe}_2] e^{Z_0}$$

$$e^{Z_0} = \text{Si}_2 \text{O}_6$$

$$\frac{\delta f}{\delta z} (\text{Si}_2 \text{O}_6) = \text{Mg}_2\text{Si}_2 \text{O}_6 + i(2\text{MgFe})_2\text{Si}_2 \text{O}_6 + i\text{Fe}_2 \text{Si}_2 \text{O}_6$$

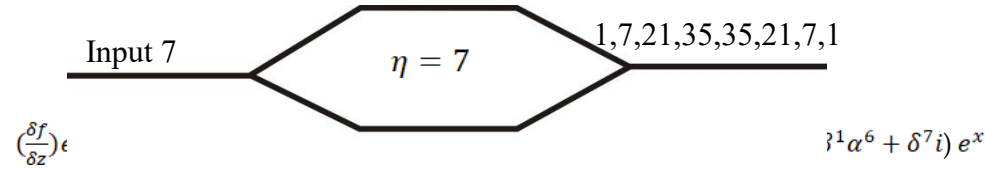
$$\frac{\delta f}{\delta z} (\text{Si}_2 \text{O}_6) = \text{Mg}_2\text{Si}_2 \text{O}_6 + i(2\text{Mgfe})_2\text{Si}_2 \text{O}_6 + i\text{Fe}_2 \text{Si}_2 \text{O}_6 \dots\dots\dots (6)$$

$$f(Z^2)e^{Z_0} = \text{Ensatite} + \text{Hypersthene} + \text{Ferrosilite}$$

Equation (6) above represents the derivatives of pyroxene series in Pascal triangle.

$$\text{Amphibole Series } (\beta + i\alpha)^\eta . e^x = (\beta_{\eta-p} \alpha_p) e^{Z_0}$$

Input the values of “ η ” in $(\beta + i\alpha)^\eta . e^x$ as $\eta = 7$, then the derivatives of Amphibole series would be generated as (1, 7, 21, 35, 35, 21, 7, 1) in the Pascal triangle.



$$= (\text{Mg}_7 + 7i\text{Mg}_6\text{Fe} + 21\text{Mg}_4\text{Fe}_2 + 35i\text{Mg}_4\text{Fe}_3 + 35\text{Mg}_3\text{Fe}_4 + 21i\text{Mg}_2\text{Fe}_5 + 7\text{MgFe}_6 + i\text{Fe}_6) e^{Z_0}$$

$$\left(\frac{\delta f}{\delta z}\right) Z_0 = [\text{Mg}_7 + 7i\text{Mg}_6\text{Fe} + 21\text{Mg}_5\text{Fe}_2 + 35i\text{Mg}_4\text{Fe}_3 + 35\text{Mg}_3\text{Fe}_4 + 21i\text{Mg}_2\text{Fe}_5 + 7\text{MgFe}_6 + i\text{Fe}_6] e^{Z_0}$$

$$e^{Z_0} = \text{Si}_8 \text{O}_{22} (\text{OH})_2.$$

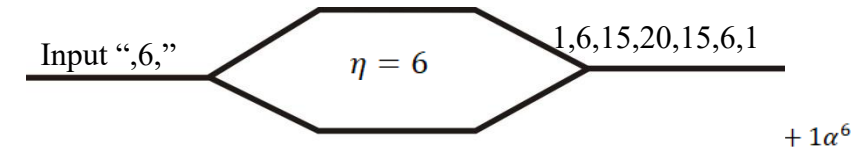
$$\left(\frac{\delta y}{\delta z}\right) \text{Si}_8 \text{O}_{22} (\text{OH})_2 = \text{Mg}_7\text{Si}_8 \text{O}_{22} (\text{OH})_2 + 7\text{Mg}_6\text{Fe Si}_8 \text{O}_{22} (\text{OH})_2 + 21\text{Mg}_5\text{Fe}_2\text{Si}_8 \text{O}_{22} (\text{OH})_2 + 35\text{Mg}_4\text{Fe}_3\text{Si}_8 \text{O}_{22} (\text{OH})_2 + 35\text{Mg}_3\text{Fe}_4\text{Si}_8 \text{O}_{22} (\text{OH})_2 + 21\text{Mg}_2\text{Fe}_5\text{Si}_8 \text{O}_{22} (\text{OH})_2 + 7\text{MgFe}_6\text{Si}_8 \text{O}_{22} (\text{OH})_2 + \text{Fe}_6\text{Si}_8 \text{O}_{22} (\text{OH})_2 \dots\dots\dots (7)$$

$$f(Z^7)e^{Z_0} = \text{Kupfferite} + (\text{Magnesio-Anthophyllite}) + (\text{Anthophyllite}) + (\text{cummingtonite} + \text{Ferro-cummingtonite}) + (\text{Grunerite})$$

Equation (7) above represents the derivatives of Amphibole series in Pascal triangle

$$\text{Mica Series } (\beta + i\alpha)^\eta . e^x = (\beta_{\eta-p} \alpha_p) e^{Z_0}.$$

Input the value of “ η ” = 6, in $(\beta + i\alpha)^\eta . e^x$ then the derivatives of Mica series would be generated as [1, 6, 15, 20, 15, 6, 1] in the Pascal Triangle.



$$\left(\frac{\delta f}{\delta z}\right) Z_0 = \text{Mg}_6 + 6i\text{Mg}_5\text{Fe} + 15\text{Mg}_4\text{Fe}_2 + 20i\text{Mg}_3\text{Fe}_3 + 15\text{Mg}_2\text{Fe}_4 + 6i\text{MgFe}_5 + \text{Fe}_6$$

$$\left(\frac{\delta f}{\delta z}\right) Z_0 = [\text{Mg}_6 + i\text{Mg}_5\text{Fe} + \text{Mg}_4\text{Fe}_2 + i\text{Mg}_3\text{Fe}_3 + \text{Mg}_2\text{Fe}_4 + i\text{MgFe}_5 + \text{Fe}_6] e^{Z_0}$$

$$e^{Z_0} = \text{Si}_8 \text{O}_{20}(\text{OH})$$

$$\left(\frac{\delta f}{\delta z}\right) \text{Si}_8 \text{O}_{20}(\text{OH}) = \text{Mg}_6 \text{Si}_8 \text{O}_{20}(\text{OH}) + i\text{Mg}_5\text{FeSi}_8 \text{O}_{20}(\text{OH}) + \text{Mg}_4\text{Fe}_2 \text{Si}_8 \text{O}_{20}(\text{OH}) + i\text{Mg}_3 \text{Fe}_3\text{Si}_8 \text{O}_{20} (\text{OH}) + \text{Mg}_2\text{Fe}_4\text{Si}_8 \text{O}_{20} (\text{OH}) + i\text{MgFe}_5\text{Si}_8 \text{O}_{20}(\text{OH}) + \text{Fe}_6 \text{Si}_8 \text{O}_{20}(\text{OH}). (8)$$

$$f(Z^6)e^{Z_0} = (\text{Phlogopite}) + (\text{Magnesio-Biotite}) + (\text{Biotite}) + (\text{Ferro-Biotite}) + (\text{Lepidomelane})$$

Equation (8) represents the derivatives of Mica series in Pascal Triangle.

Representation and Arrangement of Minerals in Pascal triangle according to Cauchy’s definition of Sequence with respect to thermodynamic conditions.

Pascal triangle is an arrangement of numbers in a triangular array such that the numbers at the end of each row are 1 and the remaining numbers are the sum of the nearest two numbers in the above row as shown in Figure (1) below. The concept is used widely in probability, combinatorics, and algebra. Pascal’s triangle is used to find the likelihood of the outcome of the toss of a coin, coefficients of binomial expansions in probability.

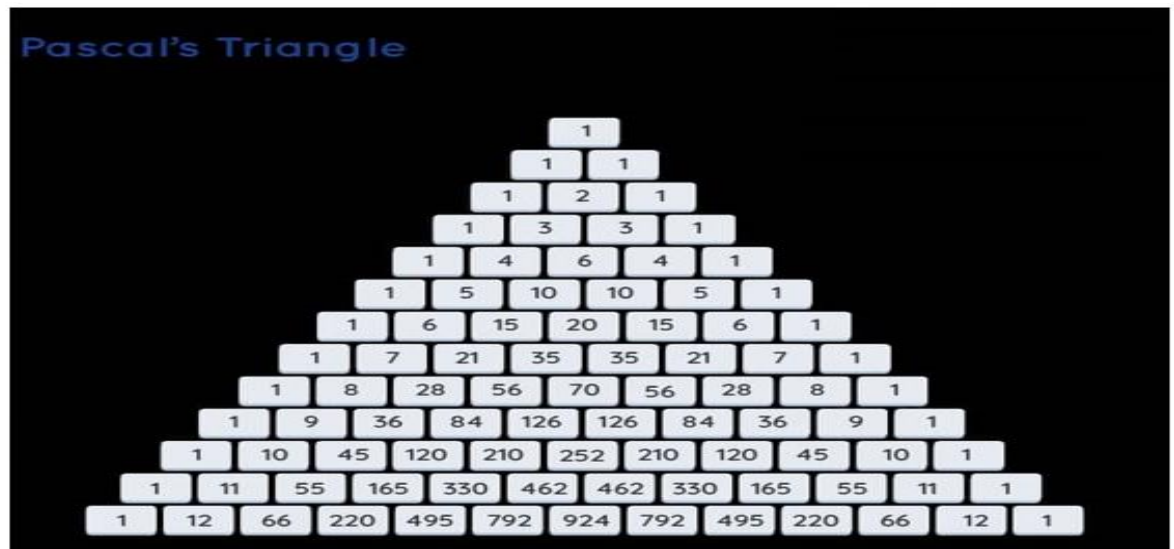
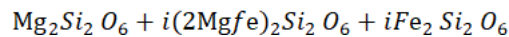


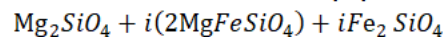
Figure 1. Pascal Tringle showing an Arrangement of Numbers in a Triangular Array

The Order of Crystallization and arrangement of Minerals under thermodynamic change can be represented in Pascal triangle using both the chemical formulas and their geologic names as shown in Figures (2) and (3) below. A: Pascal tringle Model representing Order of Crystallization and arrangement of Minerals under thermodynamic change using their chemical formulas as shown in Figure (2) below.

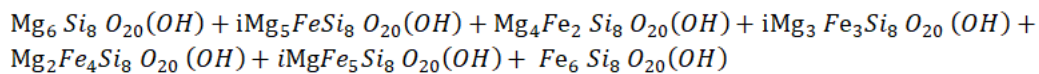
Pyroxene Series $(X + iY)^n \cdot e^x = (X_{n-p}Y_p)Z_0$



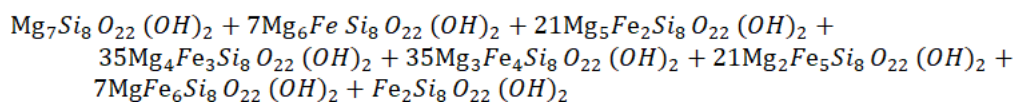
Olivine series $(\beta + i\alpha)^n \cdot e^x = (\beta_{n-p}\alpha_p)Z_0$



Mica Series $(\beta + i\alpha)^n \cdot e^x = (X_{n-p}Y_p)Z_0$.



Amphibole Series $(X + iY)^n \cdot e^x = (X_{n-p}Y_p)Z_0$



Integration in Magma, $\int w\delta z$

Integration in Magma \mathfrak{B} , is the melting of the original rocks to form magmas of different origin (\mathfrak{M}), and then into one homogenous parent magma \mathfrak{B} as shown in Equation (9)

$$\int \delta f = \int w\delta z$$

$$\int \delta f = \left[\int \frac{\delta u}{\delta x} + i \int \frac{\delta v}{\delta x} \right] + \left[i \int \frac{\delta u}{\delta y} - \int \frac{\delta v}{\delta y} \right] \dots \dots (9)$$

$$\int w\delta z = \left(\int \frac{\delta u}{\delta x} + i \frac{\delta v}{\delta x} \right) + \left(i \int \frac{\delta u}{\delta y} - \int \frac{\delta v}{\delta y} \right) \dots (10)$$

$$\boxed{\int \frac{\delta u}{\delta x} + \int \frac{\delta v}{\delta x} = -i \int \frac{\delta u}{\delta y} + \int \frac{\delta v}{\delta y}}$$

Coincidentally, using Cauchy-Riemann conditions, we have

$$\left. \begin{aligned} \int \frac{\delta u}{\delta x} = \int \frac{\delta v}{\delta y} \text{ and} \\ i \int \frac{\delta v}{\delta x} = -i \int \frac{\delta u}{\delta y} \\ \int \frac{\delta u}{\delta x} = - \int \frac{\delta u}{\delta y} \end{aligned} \right\} C \rightarrow \mathcal{R}$$

Equation (10) is called Cauchy-Riemann integral equation in magma, $\int w \delta z$.

Integration of the major Rock forming minerals $\int w \delta z$, in Magma \mathfrak{B} .

The major rock forming minerals especially the mafic series, considered are : Olivine; Pyroxene; Amphibole; Mica - Black & white micas. The integral values of Cauchy-Riemann equations are well applied in this case

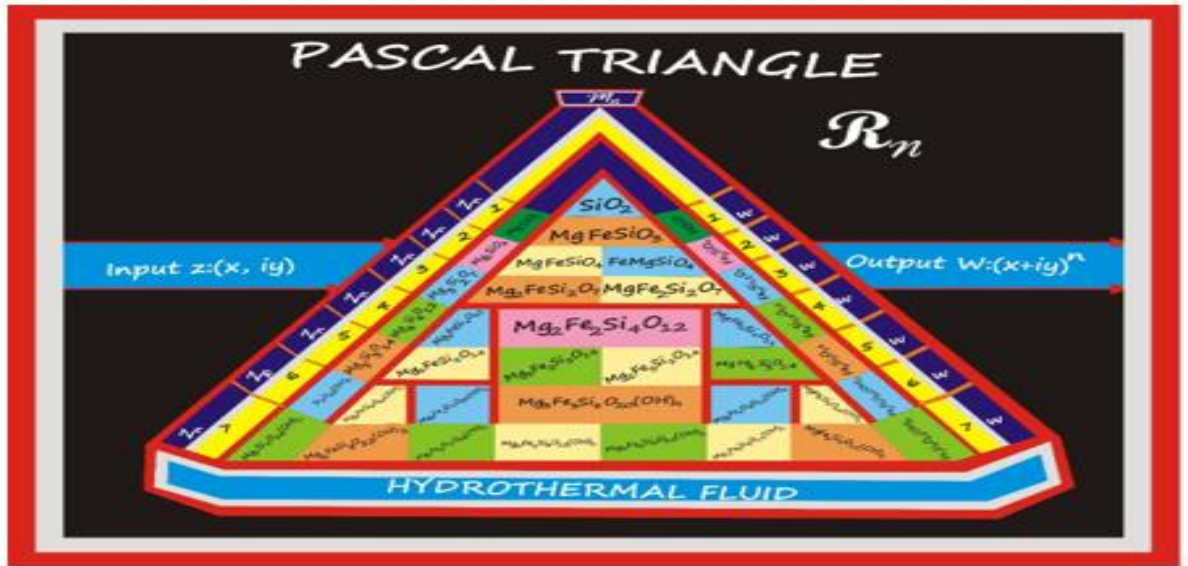


Figure 2. Pascal tringle Model representing Order of Crystallization and arrangement of Minerals under thermodynamic change using their chemical formulas.

Integration of Olivine, for $\eta = 2$

Integrate $(x + iy)^2 e^{z_0}$ using Cauchy-Riemann integral equation;

$$(x + iy)^2 e^{z_0} = (x^2 + 2xyi - y^2) e^{z_0}$$

Since,

$$f(ZZ_0) o = \omega$$

Then;

$$\omega = x^2 + 2xyi - y^2$$

$$u = x^2 - y^2$$

$$v = 2xyi$$

$$f(Z_0) o = e^{z_0}$$

$$\{ \int [w \delta z] e^{z_0} \} o = \left\{ \left[\int \frac{\delta u}{\delta x} + i \int \frac{\delta v}{\delta x} \right] + \left[i \int \frac{\delta u}{\delta y} - \int \frac{\delta v}{\delta y} \right] \left[\int e^{z_0} \right] \right\} o$$

$$\{ \int [w \delta z] e^{z_0} \} o = \left\{ \left[\int \frac{\delta}{\delta x} (x^2 - y^2) + i \int \frac{\delta}{\delta x} (2xy) \right] + \left[i \int \frac{\delta}{\delta y} (x^2 - y^2) - \int \frac{\delta}{\delta x} (2xy) \right] \right\} \int e^{z_0}$$

$$\int [w e^{z_0}] \delta z \Big|_0 = \{ x^3 + 3x^2yi - 3y^2x - iy^3 \} \{ 3Z_0 \} p \dots \dots \dots (11)$$

$$x = Mg$$

$$y = Fe$$

$$\int [\{ \beta^2 + 2\beta ai - \alpha^2 \} \{ e^{z_0} \}] \delta z = \{ \beta^3 - 3\alpha^2\beta + 3\beta^2 ai - i\alpha^3 \} \{ 3Z_0 \} p \dots \dots \dots (12)$$

$$\int [Mg_2SiO_4 + (2MgFeiSiO_4)i + Fe_2SiO_4] \delta_z = Mg_3Si_3O_9 - 3Fe_2MgSi_3O_9 - 3Mg_2FeSi_3O_9 - iFe_3Si_3O_9$$

$$\int [Mg_2SiO_4 - Fe_2SiO_4] \delta_z = Mg_3Si_3O_9 - iFe_3Si_3O_9$$

$$\int (olivine) \delta z = Mg_3Si_3O_9 - iFe_3Si_3O_9$$

$$\int (olivine) \delta z = Mg_3(SiO_3)_3 - iFe_3(SiO_3)_3$$

Si O₃ = pyroxene identity

$$\int (\text{olivine}) \delta z = \text{Pyroxene} \dots\dots\dots (13)$$

$$\int [(forstente) \delta z + (fayalite)] \delta z = \text{Enstatite} - i \text{Ferrosilite}$$

Integration of Mica, for $\eta = 6$

$$f(ZZ_0)m = \{(x + iy)^6 \cdot e^{z_0}\}m$$

Integrate $(x + iy)^6 e^{z_0}$ using Cauchy-Riemann integral equation;

$$(x + iy)^6 e^{z_0} = (x^6 + 6x^5yi + 15x^4y^2 + 2x^3y^3i + 15x^2y^4 + 6x^1y^5i + y^6) e^{z_0} \dots\dots\dots (14)$$

$$f(ZZ_0)m = (x^6 + 6x^5yi + 15x^4y^2 + 2x^3y^3i + 15x^2y^4 + 6x^1y^5i + y^6) e^{z_0}$$

Since,

$$f(ZZ_0)m = \omega$$

$$\omega = x^6 + 6x^5yi + 15x^4y^2 + 2x^3y^3i + 15x^2y^4 + 6x^1y^5i + y^6$$

$$u = x^6 + 15x^4y^2 + 15x^2y^4 + y^6$$

$$v = 6x^5y + 20x^3y^3 + 6xy^5$$

$$f(Z_0)m = e^{z_0}$$

$$1 \left\{ \int [(we^{z_0}) \delta z] m = \left[\int \frac{\delta}{\delta x} (x^6 + 15x^4y^2 + 15x^2y^4 + y^6) + i \int \frac{\delta}{\delta x} (6x^5y + 20x^3y^3 + 6xy^5) \right] \{f(e^{z_0})\} \right.$$

$$2 \left\{ \int [(we^{z_0}) \delta z] m = \left[i \int \frac{\delta}{\delta y} (x^6 + 15x^4y^2 + 15x^2y^4 + y^6) - \left[\int \frac{\delta}{\delta y} (6x^5y + 20x^3y^3 + 6xy^5) \right] \right\} \{f(e^{z_0})\}$$

For Amphibole;

$$\eta = 7$$

$$x = \beta$$

$$y = \alpha$$

$$\int \{(x + iy)^6 \cdot e^{z_0}\} \delta z = [\beta^7 + \beta^6 \alpha i + 21\beta^5 \alpha^2 + 35\beta^4 \alpha^3 i + 35\beta^3 \alpha^4 + 21\beta^2 \alpha^5 i + 7\beta \alpha^6 i + \alpha^6 i] (Z_0) a$$

... (468)

$$\int (\text{Mica}) \delta z = \{\beta^7 + \beta^6 \alpha i + 21\beta^5 \alpha^2 + 35\beta^4 \alpha^3 i + 35\beta^3 \alpha^4 + 21\beta^2 \alpha^5 i + 7\beta \alpha^6 i + \alpha^6 i\} (Z_0) a$$

Given that,

$$\beta = \text{Mg}$$

$$\alpha = \text{Fe}$$

$$e^{z_0} = \text{Si}_8\text{O}_{20}$$

$$(\int [(Mg + iFe)_6 \text{Si}_8\text{O}_{20}(\text{OH})_4] \delta z) = \text{Mg}_7\text{Si}_8\text{O}_{22}(\text{OH})_2 + i [\text{Mg}_6\text{Fe}] \text{Si}_8\text{O}_{22}(\text{OH})_2 +$$

$$[\text{Mg}_5\text{Fe}_2] \text{Si}_8\text{O}_{22}(\text{OH})_2 + i [\text{Mg}_4\text{Fe}_3] \text{Si}_8\text{O}_{22}(\text{OH})_2 + [\text{Mg}_3\text{Fe}_4] \text{Si}_8\text{O}_{22}(\text{OH})_2 +$$

$$i [\text{Mg}_2\text{Fe}_5] \text{Si}_8\text{O}_{22}(\text{OH})_2 + [\text{MgFe}_6] \text{Si}_8\text{O}_{22}(\text{OH})_2 + i [\text{Fe}_6] \text{Si}_8\text{O}_{22}(\text{OH})_2$$

..... (15)

Since $((x + iy)^7)$ is Amphibole group or series.

Then;

$$\int (\text{Mica}) \delta z = (\beta^7 + i\alpha^7) (Z_0) a$$

$$\int (\text{Mica}) \delta z = \text{Mg}_7\text{Si}_8\text{O}_{22}(\text{OH})_2 + i \text{Fe}_7 \text{Si}_8\text{O}_{22}(\text{OH})_2$$

$$\int (\text{Mica}) \delta z = (\text{Amphibole}) \dots\dots\dots (472)$$

$$\text{Amphibole} = \text{Mg}_7\text{Si}_8\text{O}_{22}(\text{OH})_2 + \text{Fe}_7\text{Si}_8\text{O}_{22}(\text{OH})_2$$

$$\text{Mica} = \text{Mg}_6\text{Si}_8\text{O}_{20}(\text{OH})_4 + \text{Fe}_6\text{Si}_8\text{O}_{20}(\text{OH})_6$$

$$[\int \text{Mg}_6\text{Si}_8\text{O}_{20}(\text{OH}) - \text{Fe}_6\text{Si}_8\text{O}_{20}(\text{OH})] \delta z = \text{Mg}_7\text{Si}_8\text{O}_{22}(\text{OH})_2 - \text{Fe}_7\text{Si}_8\text{O}_{22}(\text{OH})_2$$

$$[\int \text{Mg}_6\text{Si}_8\text{O}_{20}(\text{OH})_4 + i(\text{Fe}_6\text{Si}_8\text{O}_{20}(\text{OH})_6)] \delta z = \text{Mg}_7\text{Si}_8\text{O}_{22}(\text{OH})_2 + i(\text{Fe}_7\text{Si}_8\text{O}_{22}(\text{OH})_2). (473)$$

$$[\int w \delta z] m = [f(Z)] a \dots\dots\dots (16)$$

$$\int w \delta z = \text{Mica}$$

$$f(Z) a = \text{Amphibole}$$

$$(\int \text{pholopite} + i(\text{lepidomelane}) \delta z = \text{kupfferite} + i(\text{Grunerite}) \dots\dots\dots (17)$$

∴ The integral value of Mica in the magma, gives the Amphibole and the differential value of Amphibole would give Mica as shown in equation (17) above.



Figure 3. Pascal triangle Model representing Order of Crystallization and arrangement of Minerals under thermodynamic change using their Geologic names

Intepretation of Result

The first Bowen's index number is Forsterite of olivine, with Bowen's Index number 1(one) in the Bowen's series. 'Forsterite' under thermodynamic change, would undergo ionic substitution in the Goldschmidt space to form fayalite as the last end member of olivine in the olivine series. Both Forsterite, wholly magnesium rich olivine and Fayalite, wholly iron rich olivine are formed within the olivine series with Bowen's index number 1(one) as shown in Figure (4) below.

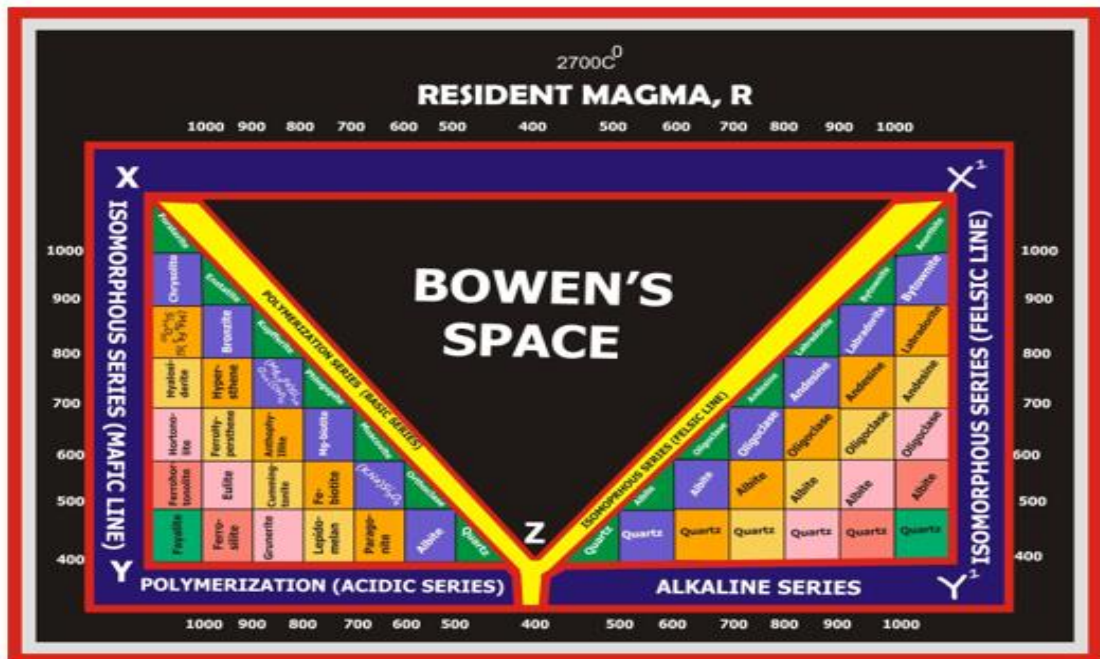


Figure 4. Mathematical Computations of Rocks in Bowen's and Goldschmidt Combined Model

The second Bowen's index number is Enstatite of pyroxene with Bowen's Index number 2(Two) in the Bowen's reaction series and the 'Enstatite' under thermodynamic change, would undergo ionic substitution in the Goldschmidt space to form Ferrosilite as the end member of pyroxene in the pyroxene series. Both Enstatite, wholly magnesium rich pyroxene and Ferrosilite, wholly iron rich pyroxene are formed within the pyroxene series with Bowen's index number

2(two) as shown Figure (4) below. The third Bowen's index number is 'Kupfferite' of amphibole with Bowen's Index number 3(Three) in the Bowen's reaction series and the 'Kupfferite' under thermodynamic change, would undergo ionic substitution in the Goldschmidt space to form Grunerite as the end member of amphibole in the amphibole series. Both Kupfferite, wholly magnesium rich amphibole and Grunerite, wholly iron rich amphibole are formed within the amphibole series with Bowen's index number 3(three) as shown in Figure (4) below. The Fourth Bowen's index number is 'Phlogopite' of mica with Bowen's Index number 4(Four) in the Bowen's reaction series and the 'Phlogopite' under thermodynamic change, would undergo ionic substitution in the Goldschmidt space to form Lepidomelane as the end member of mica in the mica series. Both Phlogopite, wholly magnesium rich mica and Lepidomelane, wholly iron rich mica are within the mica series.

Application of Partial Differential Equations (PDEs) and Integral Calculus to Rock-Forming Minerals

Partial Differential Equations (PDEs) and integral calculus are powerful mathematical tools for understanding various physical and chemical phenomena, including the study of rock-forming minerals. Their application allows us to model and analyze complex processes occurring at the micro- to macroscale within rocks (Zhang et al., 2017a); (M. J. Simpson et al., 2024).

Applications of PDEs in Mineralogy and Petrology

PDEs are used to describe how mineral properties change over time and space. Some of their main applications include (Tian et al., 2024); (M. Kang et al., 2025); (Bertozzi et al., 2025):

Diffusion in Minerals

The process of diffusion, the movement of atoms or ions through a mineral's crystal lattice, is crucial in petrology (Nixson et al., 2025); (Zhang et al., 2017b). PDEs, specifically the diffusion equation (Fick's Law), can be used to model the diffusion rates of specific elements within minerals. This helps understand the formation of zoning in minerals (changes in composition from the core to the rim), which can provide information about the thermal and pressure history of the rock. An example is the diffusion of cations in feldspar or pyroxene (Chakraborty & Dohmen, 2022); (B. Simpson et al., 2025); (Pelullo et al., 2022).

Mineral Growth and Dissolution

Crystal growth and mineral dissolution are dynamic processes that can be modeled using a PDE (Wu et al., 2024); (Rao et al., 2023); (Orosz et al., 2024). The equations describing the rate of growth or dissolution depend on the solute concentration surrounding the mineral and the thermodynamic conditions. This is relevant in the study of sedimentary rock diagenesis or metamorphism, where new minerals are formed or old minerals dissolve (Y. Kang et al., 2024).

Heat Transfer in Rocks

Temperature changes within a rock mass affect mineral stability and transformation. The heat equation (Fourier's Law), a type of PDE, is used to model heat conduction through minerals and rocks. This aids in reconstructing the cooling history of igneous or metamorphic rocks and in understanding the thermal gradients in the Earth's crust that affect mineral stability (Roberts et al., 2024); (Sun et al., 2021);(Travin et al., 2025).

Rock and Mineral Deformation

On a larger scale, PDEs can also be used to model the elastic and plastic deformation of rocks and minerals under stress (Cao et al., 2021). For example, the Navier-Stokes equations (although more commonly used for fluids, their principles can be adapted) or the elasticity equations are used in rock mechanics to understand how rocks respond to tectonic forces, which affect mineral orientation and rock structure (Dash et al., 2025).

Applications of Integral Calculus in Mineralogy and Petrology

Integral calculus, as opposed to differential calculus, allows us to sum up small effects that accumulate into a larger picture. In the context of rock-forming minerals, integrals are used to:

Calculating Mineral Volume and Mass

Knowing the density of a mineral and the function that describes its three-dimensional shape, integral calculus can be used to calculate the volume and mass of a specific mineral in a rock. This is important for modal rock analysis (the proportions of different minerals) and determining the bulk density of a rock (Zahratun et al., 2024); (Amosu & Sun, 2018); (Julianti et al., 2022).

Determining Average Concentration

If the concentration of an element varies within a mineral (e.g., zoning), integrals can be used to calculate the average concentration of that element across the mineral. This is useful in determining the bulk composition of zoned minerals (Naderloo et al., 2023); (Terron-Almenara & Panthi, 2025).

Isotope Analysis

In geochronology and the study of geological processes, integrals are used to calculate the accumulation of radiogenic isotopes over time. The radioactive decay equation is a form of integral that allows the age of rocks and minerals to be determined based on the ratio of parent and daughter isotopes.

Total Heat Flow Estimation

By integrating the heat flux over a given area, we can estimate the total heat flow through a region of the Earth's crust. This is relevant for understanding regional thermal conditions that influence mineral formation and stability.

Pressure and Temperature Reconstruction

Some mineral parameters (such as the composition of garnet or biotite) depend on the pressure and temperature at which they formed. Integrals can be used in thermodynamic models to "integrate" these compositional changes back to the initial pressure and temperature conditions under which the mineral formed.

Interactions and Synergies

Often, PDEs and integral calculus are used synergistically. For example, after solving a PDE describing the rate of diffusion of elements in a mineral, integral calculus can be used to calculate the total amount of elements that have diffused over a given time period. Or, a model constructed with PDEs for crystal growth can be integrated to predict the final crystal size. Thus, the combined use of PDEs and integral calculus provides a powerful mathematical framework for investigating the dynamics, evolution, and physical-chemical properties of rock-forming minerals, unlocking deeper insights into the geological processes that shape our planet.

Contribution

Temperature and time to establish relationships among essential rock-forming mineral, ionic charge and size to explain ionic substitutions in crystals (Diadochi) and therefore, Under mathematical context such as Partial differential equation and Integral calculus as well as other mathematical principles such as Taylor series, and Euler series with the help of thermodynamic principles, a significant documented mathematical framework complementing the explanation of Bowen's reaction series, which encompasses the ISOMORPHOUS (solid solution) and POLYMERIZATION (fractional crystallization) reaction series has been propounded using the model as shown in the Figure (4) below; Both Bowen and Goldschmidt showed a mathematical connection using Partial differential equation and Integral calculus as well as other mathematical principles such as Taylor series, and Euler series with the help of thermodynamic principles in their rules, proffering a complete mathematical explanation of rock-forming minerals and their crystallization processes using Partial differential equation and Integral calculus as well as mathematical methods such as Taylor series, and Euler series with the help of thermodynamic principles as shown in the combined model in Figure (4) below; This research achieved a holistic

understanding that bridged the gap between Bowen's and Goldschmidt's rules with a mathematical foundations such as Partial differential equation and Integral calculus.

Acknowledgments

Thanks to all parties who have supported the implementation of this research. I hope this research can be useful.

Author Contributions

Conceptualization; A. I.; methodology; L. C. I.; validation; formal analysis; H. D. B.; investigation; G. M. K.; resources; A. I.; data curation; L. C. I.; writing—original draft preparation. H. D. B.; writing—review and editing; E.; visualization; G. M. K. All authors have read and agreed to the published version of the manuscript.

Funding

Researchers independently funded this research.

Conflicts of Interest

The authors declare no conflict of interest.

Reference

- Abd El-Fatah, A. A., Surour, A. A., Azer, M. K., & Madani, A. A. (2023). Integration of Whole-Rock Geochemistry and Mineral Chemistry Data for the Petrogenesis of A-Type Ring Complex from Gebel El Bakriyah Area, Egypt. *Minerals*, 13(10), 1273. <https://doi.org/10.3390/min13101273>
- Amosu, A., & Sun, Y. (2018). MinInversion: A Program for Petrophysical Composition Analysis of Geophysical Well Log Data. *Geosciences*, 8(2), 65. <https://doi.org/10.3390/geosciences8020065>
- Bertozzi, A. L., Drenska, N., Latz, J., & Thorpe, M. (2025). Partial differential equations in data science. *Philosophical Transactions of the Royal Society A: Mathematical, Physical and Engineering Sciences*, 383(2298). <https://doi.org/10.1098/rsta.2024.0249>
- Cao, Y. J., Shen, W. Q., Shao, J. F., & Wang, W. (2021). A multi-scale model of plasticity and damage for rock-like materials with pores and inclusions. *International Journal of Rock Mechanics and Mining Sciences*, 138, 104579. <https://doi.org/10.1016/j.ijrmms.2020.104579>
- Chakraborty, S., & Dohmen, R. (2022). Diffusion chronometry of volcanic rocks: Looking backward and forward. *Bulletin of Volcanology*, 84(6). <https://doi.org/10.1007/s00445-022-01565-5>
- Chen-Charpentier, B. (2024). On Population Models with Delays and Dependence on Past Values. *Axioms*, 13(3), 206. <https://doi.org/10.3390/axioms13030206>
- Dash, S., Babu, E. V. S. S. K., Ganne, J., & Mukherjee, S. (2025). Plate tectonics through Earth's history: Constraints from the thermal evolution of Earth's upper mantle. *International Geology Review*, 67(4), 500–533. <https://doi.org/10.1080/00206814.2024.2394994>
- De Souza, A. A., Azzone, R. G., Chmyz, L., Tarazona, L. M. C., De Andrade, F. R. D., Martins, J. V., Ruberti, E., & De Barros Gomes, C. (2024). Genesis of Fe-Ti(V) Oxide-Rich Rocks by Open-System Evolution of Mafic Alkaline Magmas: The Case of the Ponte Nova Massif, SE Brazil. *Minerals*, 14(7), 724. <https://doi.org/10.3390/min14070724>
- Gutierrez-Navarro, D., & Lopez-Aguayo, S. (2018). Solving ordinary differential equations using genetic algorithms and the Taylor series matrix method. *Journal of Physics Communications*, 2(11), 115010. <https://doi.org/10.1088/2399-6528/aaedd2>
- Harnett, C. E., Kendrick, J. E., Lamur, A., Thomas, M. E., Stinton, A., Wallace, P. A., Utley, J. E. P., Murphy, W., Neuberg, J., & Lavallée, Y. (2019). Evolution of Mechanical Properties of Lava Dome Rocks Across the 1995–2010 Eruption of Soufrière Hills Volcano, Montserrat. *Frontiers in Earth Science*, 7. <https://doi.org/10.3389/feart.2019.00007>
- Hetmaniok, E., & Pleszczyński, M. (2022). Comparison of the Selected Methods Used for Solving the Ordinary Differential Equations and Their Systems. *Mathematics*, 10(3), 306. <https://doi.org/10.3390/math10030306>

- Julianti, D., Fatkhan, Dinanto, E., & Murtani, A. S. (2022). Petrophysics Analysis for Determination of Density Porosity and Neutron-Density Porosity on Carbonate Rock in East Java Basin. *IOP Conference Series: Earth and Environmental Science*, 1031(1), 012023. <https://doi.org/10.1088/1755-1315/1031/1/012023>
- Kang, M., Zhang, Z., Zhao, Z., Shi, K., Zhao, J., & Tang, P. (2025). Temporal-Spatial Partial Differential Equation Modeling of Land Cover Dynamics via Satellite Image Time Series and Sparse Regression. *Remote Sensing*, 17(7), 1211. <https://doi.org/10.3390/rs17071211>
- Kang, Y., Zhu, R., Liu, K., Zhang, J., & Zhang, S. (2024). Detrital and authigenic clay minerals in shales: A review on their identification and applications. *Heliyon*, 10(20), e39239. <https://doi.org/10.1016/j.heliyon.2024.e39239>
- Krivyakina, E., Poudel, B., Li, C., Kolesnik, S., Dabrowski, B., Mitchell, J. F., Rosenkranz, S., & Chmaissem, O. (2023). Redox Properties of Hexagonal and Cubic $\text{Sr}_{0.4}\text{Ba}_{0.6}\text{Mn}_{0.94}\text{Ti}_{0.06}\text{O}_{3-\delta}$ Investigated by In Situ Neutron Powder Diffraction. *Chemistry of Materials*, 35(15), 5895–5902. <https://doi.org/10.1021/acs.chemmater.3c00693>
- Lancellotti, L., Bianchi, A., Kovtun, A., Gazzano, M., Marforio, T. D., Xia, Z. Y., Calvaresi, M., Melucci, M., Zanardi, C., & Palermo, V. (2024). Selective ion transport in large-area graphene oxide membrane filters driven by the ionic radius and electrostatic interactions. *Nanoscale*, 16(14), 7123–7133. <https://doi.org/10.1039/d3nr05874c>
- Leung, S. C. E., Wanninayake, D., Chen, D., Nguyen, N.-T., & Li, Q. (2023). Physicochemical properties and interactions of perfluoroalkyl substances (PFAS)—Challenges and opportunities in sensing and remediation. *Science of The Total Environment*, 905, 166764. <https://doi.org/10.1016/j.scitotenv.2023.166764>
- Mourey, A. J., & Shea, T. (2019). Forming Olivine Phenocrysts in Basalt: A 3D Characterization of Growth Rates in Laboratory Experiments. *Frontiers in Earth Science*, 7. <https://doi.org/10.3389/feart.2019.00300>
- Murugesh, V., Priyadharshini, M., Sharma, Y. K., Lilhore, U. K., Alroobaea, R., Alsufyani, H., Baqasah, A. M., & Simaiya, S. (2025). A novel hybrid framework for efficient higher order ODE solvers using neural networks and block methods. *Scientific Reports*, 15(1). <https://doi.org/10.1038/s41598-025-90556-5>
- Naderloo, M., Ramesh Kumar, K., Hernandez, E., Hajibeygi, H., & Barnhoorn, A. (2023). Experimental and numerical investigation of sandstone deformation under cycling loading relevant for underground energy storage. *Journal of Energy Storage*, 64, 107198. <https://doi.org/10.1016/j.est.2023.107198>
- Nixon, R. E., Byrne, H. M., Pitt-Francis, J. M., & Maini, P. K. (2025). Characterising the Behaviour of a Structured PDE Model of the Cell Cycle in Contrast to a Corresponding ODE System. *Bulletin of Mathematical Biology*, 87(7). <https://doi.org/10.1007/s11538-025-01472-8>
- Orosz, Á., Szilágyi, E., Spats, A., Borsos, Á., Farkas, F., Markovits, I., Százdí, L., Volk, B., Kátainé Fadgyas, K., & Szilágyi, B. (2024). Dynamic Modeling and Optimal Design Space Determination of Pharmaceutical Crystallization Processes: Realizing the Synergy between Off-the-Shelf Laboratory and Industrial Scale Data. *Industrial & Engineering Chemistry Research*, 63(9), 4068–4082. <https://doi.org/10.1021/acs.iecr.3c03954>
- Pelullo, C., Iovine, R. S., Arienzo, I., Di Renzo, V., Pappalardo, L., Petrosino, P., & D'Antonio, M. (2022). Mineral-Melt Equilibria and Geothermobarometry of Campi Flegrei Magmas: Inferences for Magma Storage Conditions. *Minerals*, 12(3), 308. <https://doi.org/10.3390/min12030308>
- Peters, J. A., Djanashvili, K., Geraldes, C. F. G. C., & Platas-Iglesias, C. (2020). The chemical consequences of the gradual decrease of the ionic radius along the Ln-series. *Coordination Chemistry Reviews*, 406, 213146. <https://doi.org/10.1016/j.ccr.2019.213146>
- Racioppi, S., Hyldgaard, P., & Rahm, M. (2024). Quantifying Atomic Volume, Partial Charge, and Electronegativity in Condensed Phases. *The Journal of Physical Chemistry C*, 128(9), 4009–4017. <https://doi.org/10.1021/acs.jpcc.3c07677>
- Rao, A. R., Tide, P. S., George, Benny, K., & Mathew, J. (2023). Quasi-dynamic model for dissolution coupled with reaction and precipitation of sodium bicarbonate in fed-batch reactive crystallization. *Chemical Engineering Journal Advances*, 15, 100504. <https://doi.org/10.1016/j.cej.2023.100504>

- Roberts, N. M. W., Hernández-Montenegro, J. D., & Palin, R. M. (2024). Garnet stability during crustal melting: Implications for chemical mohometry and secular change in arc magmatism and continent formation. *Chemical Geology*, 659, 122142. <https://doi.org/10.1016/j.chemgeo.2024.122142>
- Sessa, F., & Rahm, M. (2022). Electronegativity Equilibration. *The Journal of Physical Chemistry A*, 126(32), 5472–5482. <https://doi.org/10.1021/acs.jpca.2c03814>
- Simpson, B., Ubide, T., & Spandler, C. (2025). Drivers of critical metal enrichment in peralkaline magmas recorded by clinopyroxene zoning. *Communications Earth & Environment*, 6(1). <https://doi.org/10.1038/s43247-025-02040-7>
- Simpson, M. J., Murphy, R. J., & Maclaren, O. J. (2024). Modelling count data with partial differential equation models in biology. *Journal of Theoretical Biology*, 580, 111732. <https://doi.org/10.1016/j.jtbi.2024.111732>
- Sproul, G. D. (2020). Evaluation of Electronegativity Scales. *ACS Omega*, 5(20), 11585–11594. <https://doi.org/10.1021/acsomega.0c00831>
- Sun, G., Liu, S., Cawood, P. A., Tang, M., Van Hunen, J., Gao, L., Hu, Y., & Hu, F. (2021). Thermal state and evolving geodynamic regimes of the Meso- to Neoproterozoic North China Craton. *Nature Communications*, 12(1). <https://doi.org/10.1038/s41467-021-24139-z>
- Terron-Almenara, J., & Panthi, K. K. (2025). Analysis of Plastic Deformations for Tunnel Support Design in Weak Flysch Rock Mass of a Hydropower Tunnel in Central Albania. *Rock Mechanics and Rock Engineering*, 58(7), 8111–8143. <https://doi.org/10.1007/s00603-025-04545-1>
- Tian, H., Basem, A., Kenjrawy, H. A., Al-Rubaye, A. H., Alfalahi, S. T. Y., Azarinfar, H., Khosravi, M., & Xia, X. (2024). RETRACTED: Exponential stability analysis of delayed partial differential equation systems: Applying the Lyapunov method and delay-dependent techniques. *Heliyon*, 10(12), e32650. <https://doi.org/10.1016/j.heliyon.2024.e32650>
- Travin, A., Buslov, M., Murzintsev, N., Korobkin, V., Kotler, P., Khromykh, S. V., & Zindobriy, V. D. (2025). Thermochronology of the Kalba–Narym Batholith and the Irtysh Shear Zone (Altai Accretion–Collision System): Geodynamic Implications. *Minerals*, 15(3), 243. <https://doi.org/10.3390/min15030243>
- Wu, D., Li, B., Wu, J., Hu, G., Gao, X., & Lu, J. (2024). Influence of Mineral Composition on Rock Mechanics Properties and Brittleness Evaluation of Surrounding Rocks in Soft Coal Seams. *ACS Omega*, 9(1), 1375–1388. <https://doi.org/10.1021/acsomega.3c07731>
- Zahratun, Isa, M., & Sugiyanto, D. (2024). Analysis of Mineral Types, Density, and Porosity in the Lam Teuba Formation Using Infrared Spectroscopy Method. *Jurnal Penelitian Pendidikan IPA*, 10(SpecialIssue), 24–30. <https://doi.org/10.29303/jppipa.v10ispecialissue.8115>
- Zhang, Y., Sun, H., Stowell, H. H., Zayernouri, M., & Hansen, S. E. (2017a). A review of applications of fractional calculus in Earth system dynamics. *Chaos, Solitons & Fractals*, 102, 29–46. <https://doi.org/10.1016/j.chaos.2017.03.051>
- Zhang, Y., Sun, H., Stowell, H. H., Zayernouri, M., & Hansen, S. E. (2017b). A review of applications of fractional calculus in Earth system dynamics. *Chaos, Solitons & Fractals*, 102, 29–46. <https://doi.org/10.1016/j.chaos.2017.03.051>
- Zubatyyuk, R., Smith, J. S., Nebgen, B. T., Tretiak, S., & Isayev, O. (2021). Teaching a neural network to attach and detach electrons from molecules. *Nature Communications*, 12(1). <https://doi.org/10.1038/s41467-021-24904-0>